Metallic Cylindrical EBG Structures with Defects: Directivity Analysis and Design Optimization

Halim Boutayeb, Tayeb Denidni

Metallic Cylindrical EBG Structures with Defects: Directivity Analysis and Design Optimization

Halim Boutayeb, *Member, IEEE,* and Tayeb A. Denidni, *Senior Member, IEEE*

***Abstract*— This paper presents an analysis of the directivity and the design optimization of Cylindrical Electromagnetic Band Gap (CEBG) structures constituted of metallic wires and with defects. The directivity is studied for different transversal periods, radial periods and numbers of rings. In the proposed configuration, the defects are designed by removing multiple wires, such as to form a horn-shaped aperture inside the periodic structure. From numerical results, obtained with a home-made Finite Difference Time Domain (FDTD) code, it is shown that the structures with defects present a directive beam in the stop-bands of the corresponding structures without defects. The radiation characteristics of the CEBG material are compared with those of an equivalent H-plane sectoral horn to explain the directivity mechanism. An optimization method is also proposed for minimizing the number of wires. To validate the analysis, an optimized directive antenna with a dipole as an excitation source was fabricated and measured.**

***Index Terms*— Electromagnetic bandgap materials, cylindrical structures, directive antennas.**

I. Introduction

ELECTROMAGNETIC bandgap (EBG) materials [1] have attracted a lot of interest in microwave and antenna domains because of their ability to control the propagation of electromagnetic waves. For instance, for some applications that need beam switching in only one plane, agile antennas based on reconfigurable EBG structures [2, 3] can be used to reduce the design complexity and the cost compared with adaptive antenna arrays [4] or phased array antennas [5].

Recently, Cylindrical Electromagnetic Band Gap (CEBG) structures have been introduced and used as models to develop new directive antennas or new beam switching systems [6-11]. These structures are radially and circularly periodic, and they present pass-bands and stop-bands to cylindrical electromagnetic waves. To design beam-switching antennas with CEBG materials, the technique proposed in [7-9] consists of creating defects with discontinuous wires in an initial continuous-wire structure to obtain a directive beam turning over 360° range. In [8], a multi-band reconfigurable antenna for base station applications has been presented, whereas in [6, 9], a method has been proposed to compute the transmission coefficients of CEBG structures. In [10], a configuration has been proposed for reducing the DC power supply, but this configuration has a limited narrow bandwidth. In [11], the focusing characteristics of CEBG structures have been analyzed for different defect configurations. However, in the previous work [6-11], only one value of the transversal period has been considered and the wire number has not been optimized.

The objective of this paper is to present a complete theoretical study of these CEBG materials, with defects but without active elements, for explaining the directivity mechanism and minimizing the number of wires. Indeed, for reconfigurable antenna applications, the number of required active elements and the power supply DC current can be minimized by minimizing the number of wires. Numerical simulations were carried out to compute the radiation patterns of these structures at different frequencies using the Finite Difference Time Domain (FDTD) method. A line source is used for the excitation, and the structures are considered infinite in the vertical direction.

The reminder of the paper is organized as follows. In Section II, the transmission coefficient of CEBG structures composed of metallic wires and without defect is studied for different transversal periods, radial periods and numbers of layers. In this section, the directivity of CEBG materials with defects consisting of removed wires is also analyzed. To validate the proposed analysis, experimental results for an optimized directive antenna are presented in Section III. Finally, concluding remarks are given in Section IV.

II. Analysis

In this section, the transmission coefficient of CEBG structures composed of metallic wires and without defects and the directivity of CEBG structures with defects are analysed for different transversal periods, radial periods, and numbers of rings. The effect of the wire diameter is not studied because it has a small effect when it is small compared to the operating wavelength.

A. Computation of the transmission coefficient

The CEBG structure is considered infinite in the vertical direction and is excited by an electric line source at its center. Let us consider a structure composed of $n = 3$ layers of cylindrical periodic surfaces of metallic wires, as shown in Fig. 1(a). The cylindrical surfaces are periodically spaced with the period P_r and have the same transversal period P_t, and accordingly the same transmission and reflection coefficients (t and r) [9]. The transversal period is kept constant by modifying adequately the angular period of each layer ($P_{\varphi i} = P_{\varphi 1}/i$). The diameter of the wires is a. We also denote by N_i ($N_i = 360/P_{\varphi i} = N_1 i$) the number of wires in each layer. The total number of wires is given by

$$N_{tot} = \frac{360}{P_{\varphi 1}} \Sigma_{i=1}^{i=n} i = N_1 \frac{(n+1)n}{2} \qquad (1)$$

Manuscript received December 12, 2006. This work was supported by the National Science Engineering Research Council of Canada (NSERC).

The authors are with INRS-Télécommunications, University of Quebec, 800 rue de la Gauchetiere, Montreal, Quebec H5A 1K6, Canada. boutayeb@emt.inrs.ca

The propagation of the transverse electric field in the radial direction is considered. According to [9], considering single-mode interactions between layers, the transmission and reflection coefficients of the structure with n cylindrical shells can be written as

$$t_n = \frac{t_{n-1}t}{1 - r_{n-1}re^{-j2\eta_0(knP_r))+j2\eta_0(k(n-1)P_r)}} \quad (2)$$

$$r_n = r_{n-1} + \frac{t_{n-1}^2 re^{-j2\eta_0(knP_r))+j2\eta_0(kP_r)}}{1 - r_{n-1}re^{-j2\eta_0(knP_r))+j2\eta_0(k(n-1)P_r)}} \quad (3)$$

where $t_1 = t$, $r_1 = r$, k is the free space wave number and $\eta_0(x)$ is the phase of the cylindrical wave:

$$\eta_0(x) = arctan\left(\frac{N_0(x)}{J_0(x)}\right) \quad (4)$$

where $J_0(x)$ and $N_0(x)$ are the first and second kind Bessel functions of zero order.
The coefficients t and r of a cylindrical shell were calculated by using the same extraction method proposed in [6, 9].

B. Computation of the directivity

While the previous subsection has presented the analysis method for the CEBG structures without defect, the technique to compute the directivity of materials with defects is now described. The defects are introduced by removing wires forming a horn-shaped aperture inside the periodic structure. Figure 3 (a) shows the geometry of a structure with defects. It is illuminated by an infinite current line source, placed in its center. Finite Difference Time Domain (FDTD) simulations using a home-made code were carried out to compute the radiation characteristics of the structure. In these FDTD simulations, the wires are modeled using Holland and Simpson thin-wire formalism [12], without charge variation, a Gaussian pulse is used, and electric walls are used in the vertical direction. The far-field proprieties are investigated through an examination of the two-dimensional directivity at $\varphi = 0°$:

$$D_{CEBG} = 10\log\left(\frac{2\pi|E_z(\varphi=0)|^2}{\int_0^{2\pi}|E_z(\varphi)|^2 d\varphi}\right) \quad (5)$$

where E_z is the transverse component of the total electric field in the far region.
For comparison, the 2-D directivity of an equivalent H-plane sectoral horn antenna is also computed. The H-plane pattern of the horn antenna can be calculated numerically from the following relation [13]:

$$F(\varphi) = \frac{1+\cos\varphi}{2}\int_{-\frac{A}{2}}^{\frac{A}{2}} \cos\left(\frac{\pi x}{A}\right) e^{-jk(\sqrt{(R^2+x^2)}-x\sin\varphi)} dx \quad (6)$$

where A and R parameters are defined as illustrated in Fig. 6. The 2-D directivity is calculated from :

$$D_{Horn} = 10\log\left(\frac{2\pi|F(\varphi=0)|^2}{\int_0^{2\pi}|F(\varphi)|^2 d\varphi}\right) \quad (7)$$

C. Effect of the transversal period

The number of layers and the radial period are fixed, and the transversal period is varied. The following values for the angular period of the first layer are considered $P_{\varphi 1} = 20°$, $30°$, $40°$ and $60°$.

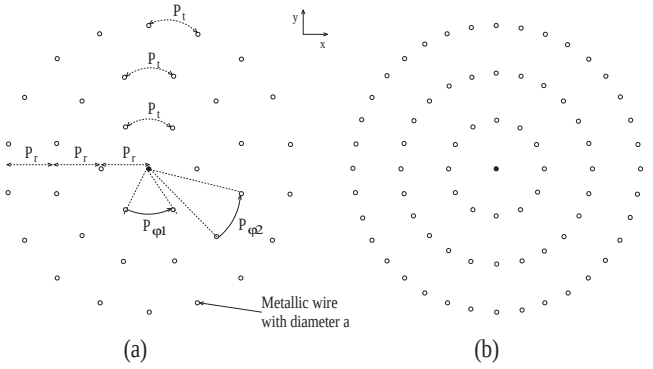

Fig. 1. CEBG structures without defect, with fixed radial period P_r and number of wires $n = 3$, for different transversal periods (a) $P_{\varphi 1} = 60°$. (b) $P_{\varphi 1} = 30°$.

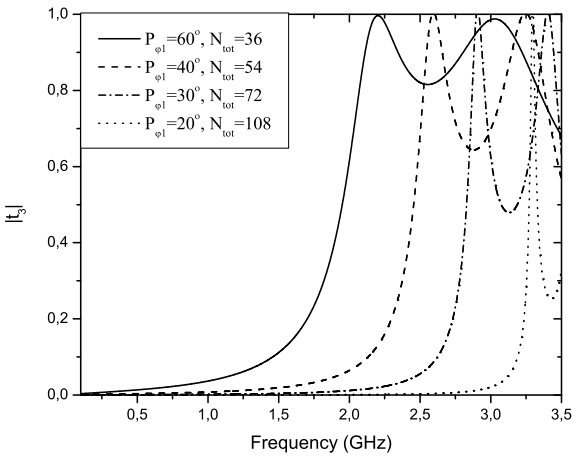

Fig. 2. Transmission coefficients of CEBG structures with three layers and fixed radial period for different transversal periods.

Note that the cases $P_r < P_t$ are not considered because higher modes can be excited for these cases and the analytical model based on a single-mode becomes not accurate. From this, the maximum angular period considered here is $P_{\varphi 1} = 60°$. Figure 1 shows two examples of structures without defects for $P_{\varphi 1} = 60°$ and $P_{\varphi 1} = 30°$. The following parameters are considered: $P_r = 40\ mm$, $n = 3$ and $a = 2\ mm$. Figure 2 presents the transmission coefficient of the CEBG structure for different values of $P_{\varphi 1}$. From this figure, at low frequencies, P_r is near 0 compared to the wavelength λ. At the stop-band upper end, P_r is near 0.3λ for large transversal period ($P_{\varphi 1} = 60°$) and near 0.4λ for small transversal period ($P_{\varphi 1} = 20°$). From this, the stop-band condition is $0.3\lambda < P_{r,max} < 0.4\lambda$. As a result, by decreasing the transversal period, the stop-band

increases.

The same structures but with defects, as illustrated in Fig. 3, are now considered. Note that if no defect is created, the radiation patterns are omnidirectional. Figure 4 presents the calculated directivity for the different cases. From these curves, it can be noted that the directivity increases with frequency until a certain frequency that is related to the stop-band upper-end of the corresponding structure without defect (see Fig. 2). One can also note that, when the period is decreased, the directivity does not change in the stop-band. This is due to the fact that, for sufficiently small transversal period, the periodicity is not seen by electromagnetic waves.

As an example, Fig. 5 presents the radiation patterns of the structure in Fig. 3(a) at different frequencies. From these patterns, it can be noted that a unique directive main beam is obtained in the stop-band. In the pass-band, the back radiation becomes as important as the main beam, which explains the directivity change. Within the stop-band, the increasing of directivity with frequency is due to the increasing of the radiation aperture size in terms of wavelengths.

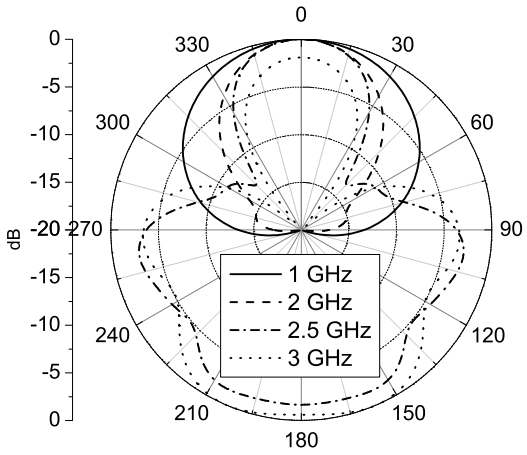

Fig. 5. Radiation patterns of the CEBG structure in Fig. 3(a) at different frequencies. The frequencies $1GHz$ and $2GHz$ belong to the stop-band. The frequencies $2.5GHz$ and $3GHz$ belong to the pass-band.

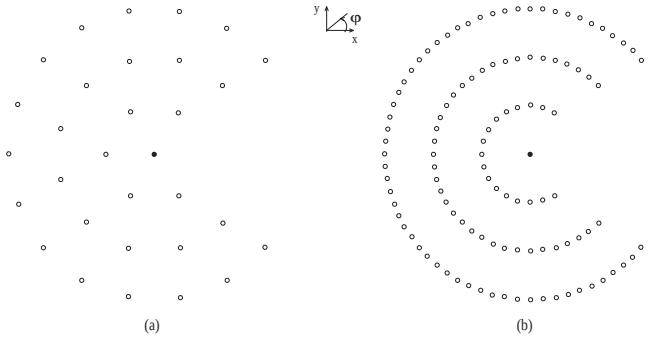

Fig. 3. CEBG structures with defects, with fixed radial period P_r and $n = 3$, for different transversal periods (a) $P_{\varphi 1} = 60°$. (b) $P_{\varphi 1} = 15°$.

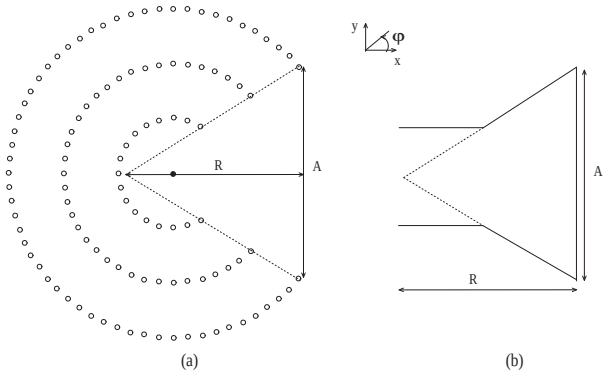

Fig. 6. (a) CEBG structure with defect and $P_{\varphi 1} = 15°$ (b) H-plane sectoral horn antenna with the same shape as the defect.

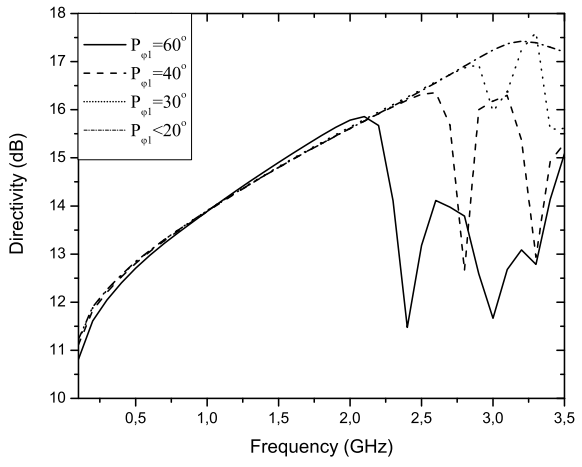

Fig. 4. Directivity at $\varphi = 0°$ for structures with three layers and fixed radial period, for different transversal periods.

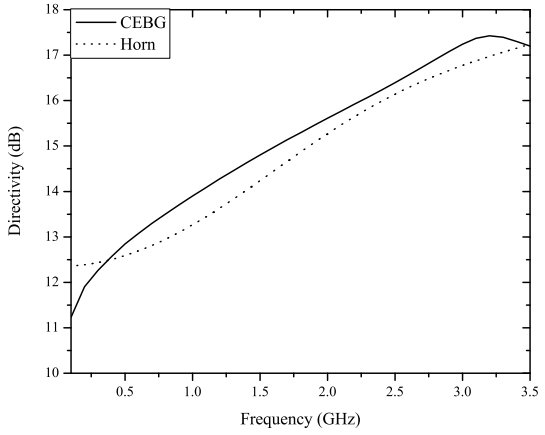

Fig. 7. Directivities at $\varphi = 0°$ of a CEBG structure with $P_{\varphi 1} = 15°$ and of an equivalent horn structure (see Fig. 6).

To explain further the directivity mechanism, Fig. 7 compares the directivities of the CEBG structure and of a horn with

the same shape (see Fig. 6). Theses results show that the directivities are close to each other, but the CEBG material is slightly more directive, probably because diffracted fields at the edge are lower for this structure than for the horn [14]. As a conclusion, the directivity bandwidth of the CEBG structure is directly related to the stop-band upper-end of the structure without defect, and within the stop-band, the CEBG structure with defects acts as a horn. To increase the directivity bandwidth, the transversal period can be decreased, but this conducts to increasing the number of wires. In the next subsection, another method to increase this bandwidth with less number of wires is presented.

D. Effect of the radial period

In this subsection, the size of the CEBG structure and the angular period of the first layer are fixed ($P_{\varphi 1} = 60°$), whereas the number of layers and the radial period are varied adequately to keep the same outer diameter (the parameter $2nP_r$ is constant). Figure 8 shows two structures without defect that follow these specifications for $n = 3$ ($P_r = 40$ mm) and $n = 5$ ($P_r = 24$ mm).

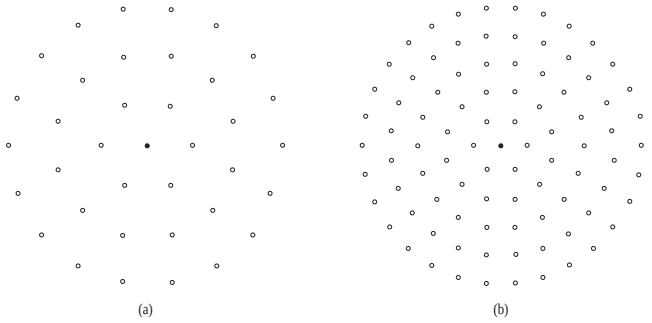

Fig. 8. CEBG structures without defect, with fixed outer diameter and $P_{\varphi 1} = 60°$, for different number of layers (a) $n = 3$, $P_r = 40$ mm. (b) $n = 5$, $P_r = 24$ mm.

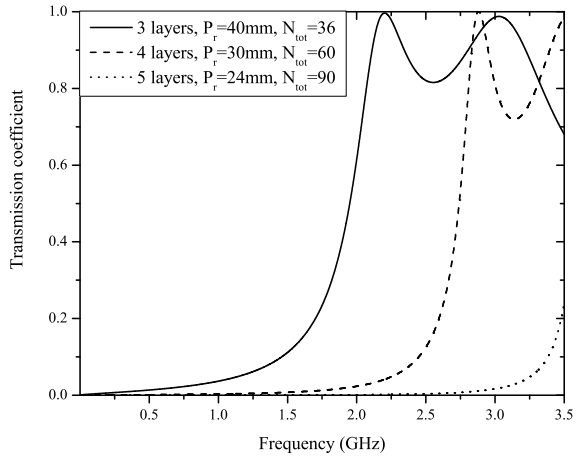

Fig. 9. Transmission coefficients for structures with fixed outer diameter and fixed $P_{\varphi 1} = 60°$, for different number of layers.

Figure 9 presents the transmission coefficient obtained for $n = 3$ to 5. From these curves, it can be seen that the stop-band increases if the radial period decreases and the stop-band condition $P_r < P_{r,max} \approx 0.3\lambda$ is maintained.

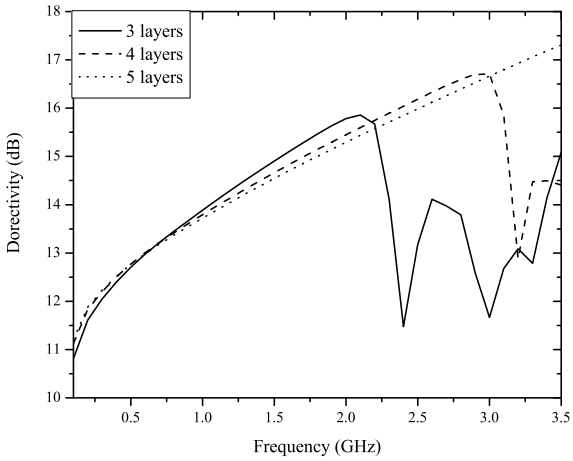

Fig. 10. Directivity at $\varphi = 0°$ for structures with fixed outer diameter and fixed $P_{\varphi 1} = 60°$, for different numbers of layers.

The computed directivity for the structures with defects is plotted in Fig. 10, confirming that the directivity bandwidth is related to the stop-band of the structures without defect (see Fig. 9). It can be noted also that the directivity bandwidth increases faster with the number of wires than in the previous subsection (*i.e.* by decreasing the transversal period). For example, the structure with $P_r = 24mm$ and $n = 5$ presents a stop-band until $3.5GHz$ (see Fig. 9), with $N_{tot} = 90$, whereas the structure with $P_{\varphi 1} = 20°$ and $n = 3$ presents a stop-band until 3.25 GHz (see Fig. 2), with $N_{tot} = 108$. As a conclusion, for minimizing the number of wires and increasing the directivity bandwidth, it is more judicious operation to decrease the radial period than the transversal period. From this, we choose the optimized angular period $P_{\varphi 1} = 60°$.

E. Effect of the number of layers

In this subsection, the radial period and the transversal period of the CEBG structure are fixed ($P_r = 40$ mm , $P_{\varphi 1} = 60°$) and the number of layers is varied, which increases the structure size. Note that the optimized configuration $P_{\varphi 1} = 60°$ is considered to minimize the number of wires.

Figure 11 presents the transmission coefficient of CEBG structures for different numbers of rings. It can be seen that, for the structure with one layer there is no resonant frequency. It can be noted also that increasing the number of layers decreases slightly the stop-band.

The directivity of structures with defects is presented in Fig. 12. As observed in Fig. 11 for the transmission coefficient, the directivity bandwidth decreases slightly when the number of layers increases. For one layer, the maximum of directivity is obtained around the middle of the pass-band. As expected, within the stop-band, the directivity increases according to the

size of the structure. At the frequency where the enhancement of directivity is maximum, around 2 GHz, the directivity increases by 2 dB when the size is doubled.
It should be noted that if the number of layers is increased further, the defect configuration should be modified in order to maximize the directivity. According to the previous results, the defect configuration design can be facilitated by designing first the equivalent horn.

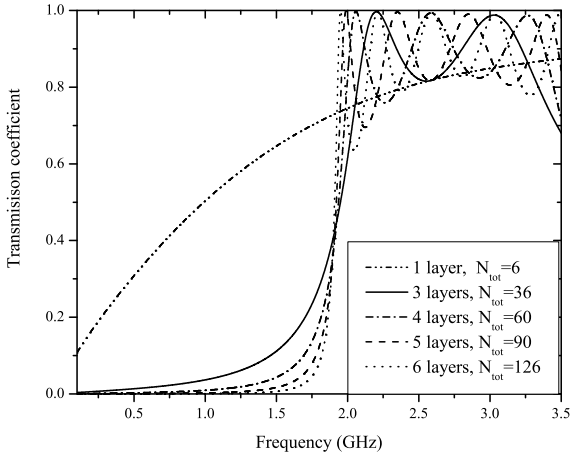

Fig. 11. Transmission coefficients for structures with fixed radial period $P_{\varphi 1} = 60°$, for different numbers of layers.

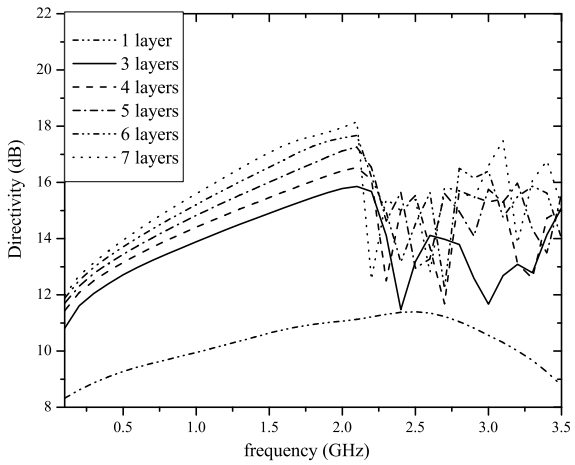

Fig. 12. Directivity at $\varphi = 0°$ for structures with fixed radial period and fixed $P_{\varphi 1} = 60°$, for different numbers of layers.

III. Experimental results

To validate the proposed analysis, an optimized (*i.e.* with minimum number of wires) CEBG antenna prototype was fabricated. Figure 13 shows the side view of the antenna and its photograph is shown in Fig. 14. A dipole is used as an excitation source and two metallic cones are on both sides of each wire, to improve the radiation pattern in the E-plane (vertical plane). The CEBG structure is composed of $n = 4$ layers, the wire diameter is $a = 1.5\ mm$, the radial period is $P_r = 38\ mm$ and the angular period of the first layer is $P_{\varphi 1} = 60°$ (the top-view is given by Fig. 3(a), except $n = 4$). The directivity frequency limit is around 2.3 GHz.

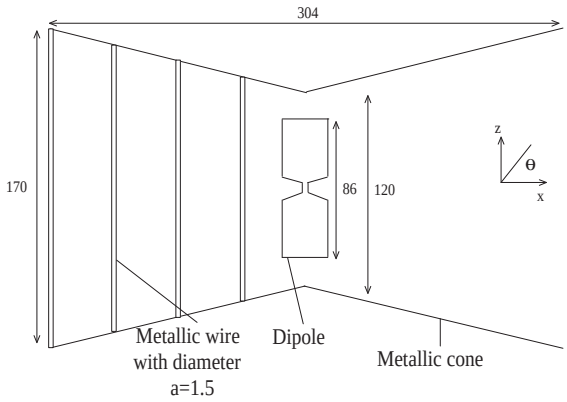

Fig. 13. Side view of the fabricated optimized CEBG directive antenna (dimensions in *mm*).

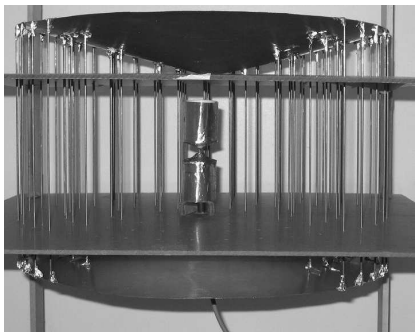

Fig. 14. Photograph of the fabricated CEBG antenna.

Figure 15 presents the simulated radiation patterns of the antenna at 2.2 GHz, with and without the metallic cones. Theses results show that the metallic cones improve the radiation patterns in both planes. The greater improvement is observed in the E-plane.
The measured return loss of the antenna is shown in Fig. 16. The bandwidth of the antenna is the intersection between the impedance bandwidth ($S_{11} < -10dB$) and the directivity bandwidth, which is fixed by the radial period of the CEBG structure ($f < 2.3\ GHz$). From these, the antenna offers a bandwidth from 2.06 GHz to 2.3 GHz. The measured patterns are shown in Fig. 17, at 2.2 GHz. From these results, the half-power beamwidth are 39° and 50.4°, in the E-plane and H-plane, respectively. In the operating band, the antenna gain is around 13 dB. According to Section II, the gain of the antenna can be enhanced by increasing the number of layers. There are slight differences between measured (Fig. 17) and simulated (Fig. 15) radiation patterns, due to fabrication tolerances.

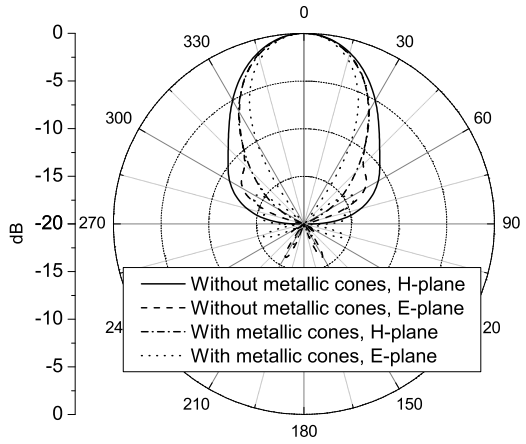

Fig. 15. Simulated radiation patterns of the CEBG antenna at 2.2 GHz.

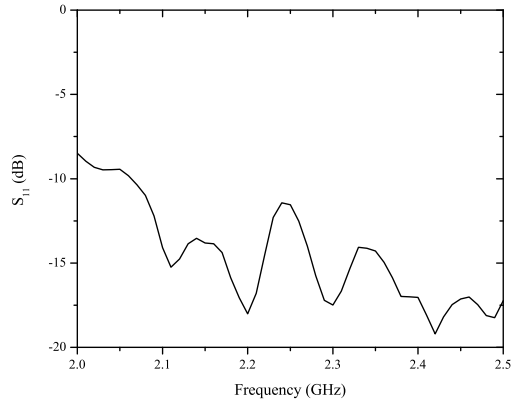

Fig. 16. Measured return loss of the fabricated CEBG antenna.

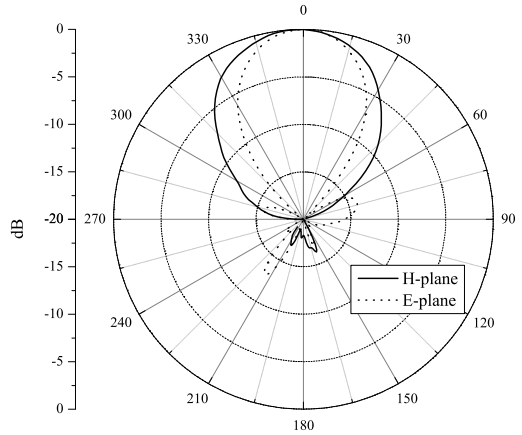

Fig. 17. Measured Co-pol radiation patterns in the H- and E-planes at 2.2 GHz (X-pol are lower than -20 dB).

IV. Conclusion

The directivity analysis and the design optimization of Cylindrical Electromagnetic Band Gap (CEBG) materials constituted of metallic wires and with defects have been presented. It is shown that within the stop-band of the structure without defects, the CEBG structure with defects acts as a horn. The relationship between the directivity bandwidth and the radial period has also been presented. In addition, a method is proposed to minimize the number of wires. To validate the proposed analysis, experimental results for an optimized CEBG antenna have been presented.

References

[1] J. Joannopoulos, R. D. Meade and J. N. Winn, *Photonic crystals: molding the flow of light*, Princeton, NJ: Princeton Univ. Press, 1995.

[2] J.M. Lourtioz , A. De Lustrac, F. Gadot, S. Rowson, A. Chelnokov, T. Brillat, A. Ammouche, J. Danglot, O. Vanbesien, and D. Lippens, "Toward controllable photonic crystals for centimeter and millimeter wave devices", *J. Lightwave Tech.*, vol. 17, pp. 2025-2031, Nov. 1999.

[3] G. Poilasne, P. Pouliquen, K. Mahdjoubi, L. Desclos and C. Terret, "Active metallic photonic bandgap material MPBG: experimental results on beam shaper", *IEEE Trans. Ant. Prop.*, vol. 48, pp. 117-119, Jan. 2000.

[4] R. T. Jr. Compton, *Adaptive Antennas: Concepts and Performance*, Englewood Cliffs, NJ: Prentice-Hall, 1988.

[5] R. J. Mailloux, *Phased Array Antenna Handbook*, Boston, MA: Artech House, 1994.

[6] H. Boutayeb, K. Mahdjoubi, and A.C. Tarot, "Analysis of radius-periodic cylindrical structures", in *Proc. IEEE AP-S Int. Symp. Dig.*, vol. 2, pp. 813- 816, June 2003.

[7] H. Boutayeb, "Étude des structures périodiques planaires et conformes associées aux antennes. Application aux communications mobiles"(in french), *Ph.D thesis, University of Rennes, France*, Dec. 2003.

[8] P. Ratasjack, T. Brillat, F. Gadot, P.Y. Garel, A. de Lustrac, H. Boutayeb, K. Mahdjoubi, A.C Tarot, and J.P. Daniel, "A reconfigurable EBG structure for a beam steering base station antenna", *JINA*, Nov. 2004.

[9] H. Boutayeb, T. A. Denidni, K. Mahdjoubi, A.-C. Tarot, A. Sebak and L.Talbi, "Analysis and Design of a Cylindrical EBG-based directive antenna", *IEEE Trans. Ant. Prop.*, vol. 54, pp. 211-219, Jan. 2006.

[10] H. Boutayeb and T. A. Denidni, "Technique for Reducing the Power Supply in Reconfigurable Cylindrical Electromagnetic Band Gap Structures", *IEEE Ant. Wir. Prop. Lett.*, vol. 5, pp. 425-425, 2006.

[11] H. Boutayeb, A.-C. Tarot, and K. Mahdjoubi, "Focusing Characteristics of a Metallic Cylindrical Electromagnetic Band Gap Structure with Defects", *Progress in Electromagnetic Research*, vol. 66, pp. 89-103, 2006

[12] H. Holland and L. Simpson "Finite-diference analysis of EMP coupling to thin struts and wires", *IEEE Trans. Electromagn. Compat.*, vol. 23, pp.88-97, May 1981.

[13] W. L. Stutzman and G. Thiele, *Antenna theory and design*, 2nd Ed., New York, John Wiley & Sons, pp. 300-304, 1998.

[14] R.E, Lawrie, L. Peters, Jr.,"Modifications of horn antennas for low sidelobe levels", *IEEE Trans. Ant. Prop.*, vol. 14, pp. 605-610, Sep. 1966.